J. Fluid Mech. (1992), *vol.* 244, *pp.* 1–16

Effect of nonlinear polarization on shapes and stability of pendant and sessile drops in an electric (magnetic) field

By OSMAN A. BASARAN[1] AND FRED K. WOHLHUTER[2]

[1] Chemical Technology Division, Oak Ridge National Laboratory, Oak Ridge, TN 37831-6224, USA

[2] Department of Chemical Engineering, University of Tennessee, Knoxville, TN 37996, USA

(Received 13 November 1991 and in revised form 12 March 1992)

Axisymmetric shapes and stability of nonlinearly polarizable dielectric (ferrofluid) drops of fixed volume which are pendant/sessile on one plate of a parallel-plate capacitor and are subjected to an applied electric (magnetic) field are determined by solving simultaneously the free boundary problem comprised of the Young–Laplace equation for drop shape and the Maxwell equations for electric (magnetic) field distribution. Motivated by the desire to explain certain experiments with ferrofluids, a constitutive relation often used to describe the variation of polarization with applied field strength is adopted here to close the set of equations that govern the distribution of electric field. Specifically, the nonlinear polarization, P, is described by a Langevin equation of the form $P = \alpha[\coth(\tau E) - 1/(\tau E)]$, where E is the electric field strength. As expected, the results show that nonlinearly polarizable drops behave similarly to linearly polarizable drops at low field strengths when drop deformations are small. However, it is demonstrated that at higher values of the field strength when drop deformations are substantial, nonlinearly polarizable supported drops whose contact lines are fixed, as well as ones whose contact angles are prescribed, display hysteresis in drop deformation over a wide range of values of the Langevin parameters α and τ. Indeed, properly accounting for the nonlinearity of the polarization improves the quantitative agreement between theory and the experiments of Bacri *et al.* (1982) and Bacri & Salin (1982, 1983). Detailed examination of the electric fields inside nonlinearly polarizable supported drops reveals that they are very non-uniform, in contrast to the nearly uniform fields usually found inside linearly polarizable drops.

1. Introduction

In the presence of an applied electric (magnetic) field, a supported – pendant or sessile – or a free drop of a dielectric (magnetic) liquid elongates in the direction of the applied field. The form of the equations that govern the response of a drop of dielectric liquid in an applied electric field is the same as those that govern the response of a drop of magnetic liquid, or ferrofluid, in an applied magnetic field (cf. Rosensweig 1979, 1985; Melcher & Taylor 1969; Melcher 1981). Therefore, conclusions made in the context of the problem of a drop in an electric field, as in this paper, apply equally well to the magnetic problem.

Theoretical analyses, such as that due to Rosenkilde (1969) and Berkovsky & Kalikmanov (1985), approximated drop shapes in externally applied fields as

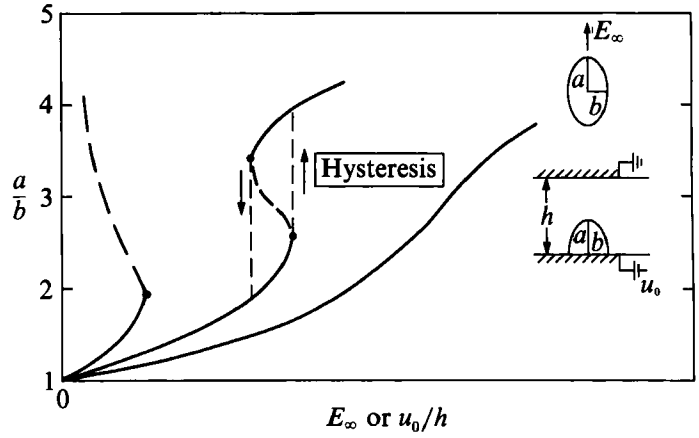

FIGURE 1. Three possible ways that the equilibrium aspect ratio a/b of a free or supported drop can vary as a function of the dimensionless field strength. In the case of a free drop, E_∞ is the uniform field strength infinitely far away from the drop. In the case of a supported drop, one electrode is at potential u_0 and the other electrode, a distance h from it, is grounded. ——, Stable; – – –, unstable; •, turning point.

spheroids. Through such approximations, these authors surmized that liquid drops can respond in one of three qualitative ways that depend on the ratio of the permeability of the drop to that of the surrounding fluid, κ: see figure 1. Most remarkably, as shown in figure 1, these analyses predicted that for certain values of κ, drop deformation can exhibit hysteresis. The possibility of hysteresis has been confirmed in laboratory experiments by Bacri, Salin & Massart (1982) and Bacri & Salin (1982, 1983). Unfortunately, rigorous numerical calculations by Miksis (1981), Sherwood (1988), and Cheng & Miksis (1989) have been unable to demonstrate the occurrence of hysteresis. Theoretical prediction of if and when supported drops can exhibit hysteresis in deformation under the influence of an applied electric (magnetic) field is a major goal of this paper.

Recently, Wohlhuter & Basaran (1992, hereinafter referred to as W & B), (i) provided a thorough and critical analysis of previous work in this area and (ii) analysed the axisymmetric shapes and stability of *linearly* polarizable dielectric drops that are surrounded by another linearly polarizable dielectric and are pendant or sessile on a face of a parallel-plate capacitor. W & B showed that hysteresis can occur, but the range of values of κ over which it occurs is quite narrow and is strongly dependent on the boundary condition at the three-phase contact line where the drop, the surrounding fluid, and the solid plate meet. However, the theoretical prediction of W & B of the case corresponding to the experiments of Bacri and coworkers differed from the experimental measurements by a factor of two. W & B showed that some, but not all, of the differences between the theory and the experiments could be attributed to the method of estimating κ in the experiments and also to the use of suspensions of drops instead of single drops of ferrofluid in the experiments. Another major goal of this paper is to resolve completely this long-standing discrepancy between theory and experiment.

The pioneering approximations of Rosenkilde (1969) and others and the more recent, rigorous calculations of Miksis (1981), Sherwood (1988), Cheng & Miksis (1989), and W & B have all assumed the drops to be linearly polarizable materials. For such materials, the relationship between the induced polarization (or magnetization) and the applied field is independent of field strength. However,

magnetic liquids in particular (e.g. Rosensweig 1979, 1985) and dielectric liquids at large field strengths are *nonlinearly* polarizable, i.e. the constant of proportionality between the polarization and the applied field is field dependent. To date, only Boudouvis, Puchalla & Scriven (1988) have made calculations that account for the nonlinear polarization of the drop material. They presented results for only one case which modelled and agreed with their experimental measurements, and the parameters they used to describe the nonlinear magnetization of their drop fluid were such that only a monotonically increasing deformation curve resulted.

Section 2 of this paper presents the equations and boundary conditions that govern the equilibrium shapes and stability of a nonlinearly polarizable dielectric drop on a face of a circular parallel-plate capacitor. Because the electric field in the drop is governed by a nonlinear Maxwell equation, boundary-integral techniques such as those used by Miksis (1981) cannot be used to determine the field inside the drops. Therefore, the computational techniques developed in W & B for drops that are linearly polarizable dielectrics are extended to analyse situations in which the drop material is nonlinearly polarizable. Section 3 presents solution families, drop shapes, and potential and electric fields computed from the theoretical analysis. Finally, in §4 these results are compared to experimental results reported by Bacri *et al.* (1982) and Bacri & Salin (1982, 1983), and theory and experiment are at last brought into accord.

2. Mathematical formulation

2.1. *Fundamental equations for nonlinearly polarizable materials*

An axisymmetric drop of a nonlinearly polarizable dielectric of permittivity ϵ_b surrounded by a linearly polarizable fluid insulator of permittivity ϵ_a sits on or hangs from, i.e. is sessile on or pendant from, one face of a circular parallel-plate capacitor of radius large compared to the distance h between the plates, as shown in figure 2. Here, $\epsilon_b = \epsilon_b(\tilde{E}^2)$, where $\tilde{\boldsymbol{E}}$ is the electric field, and ϵ_a is a constant for a given material. The surface tension of the drop/ambient fluid interface is σ. One plate of the capacitor is at potential u_0, relative to the other, which is grounded. The electric field inside and outside the drop is governed by Maxwell's equations:

$$\tilde{\nabla}\cdot\tilde{\boldsymbol{D}} = 0, \tag{1}$$

$$\tilde{\nabla}\times\tilde{\boldsymbol{E}} = \boldsymbol{0}. \tag{2}$$

Equations (1) and (2) are Gauss's/Coulomb's and Faraday's laws respectively, and the electric displacement $\tilde{\boldsymbol{D}}$ is related to the electric field and the fluid polarization $\tilde{\boldsymbol{P}}$ by

$$\tilde{\boldsymbol{D}} = \epsilon\tilde{\boldsymbol{E}} = \epsilon_0\tilde{\boldsymbol{E}} + \tilde{\boldsymbol{P}}, \tag{3}$$

where ϵ_0 is the permittivity of free space. The Maxwell equations (1) and (2) are not closed until a constitutive relation is specified between the polarization and the electric field: this point is returned to below. In the simplest case, the polarization can be taken parallel to the electric field, i.e.

$$\tilde{\boldsymbol{P}} = \frac{\tilde{P}}{\tilde{E}}\tilde{\boldsymbol{E}}. \tag{4}$$

For ferrofluids, the fluid polarization or magnetization $\tilde{\boldsymbol{M}}$ is also collinear with the magnetic field $\tilde{\boldsymbol{H}}$: such materials are known as soft materials (e.g. Rosensweig 1985).

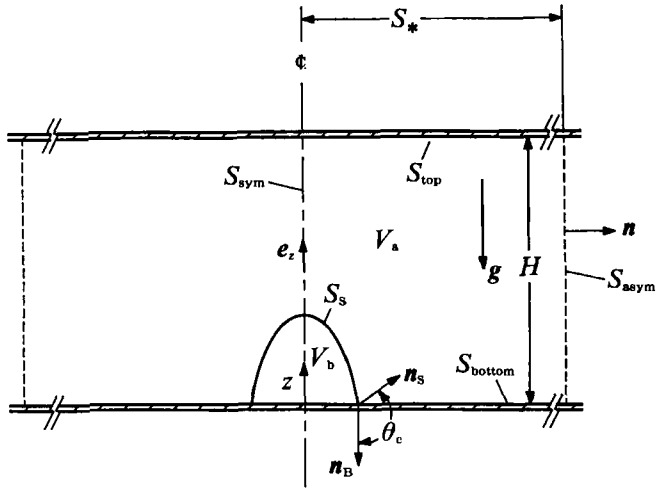

FIGURE 2. Axisymmetric dielectric drop on a face of a circular parallel-plate capacitor.

The stress tensor for a nonlinearly polarizable, incompressible fluid for which $\tilde{\boldsymbol{P}} \| \tilde{\boldsymbol{E}}$ and at constant temperature is (see e.g. Rosensweig 1985; Basaran 1984)

$$\tilde{\boldsymbol{T}} = -\left[\tilde{p} + \int_0^{\tilde{E}} \tilde{P}(\tilde{E}')\,\mathrm{d}\tilde{E}' + \tfrac{1}{2}\epsilon_0 E^2\right]\boldsymbol{I} + \tilde{\boldsymbol{D}}\tilde{\boldsymbol{E}}, \tag{5}$$

where $\tilde{p}$ is the sum of ordinary and electrostrictive pressures. For a linearly polarizable fluid, (5) reduces to the familiar form given in standard texts (e.g. Landau & Lifshitz 1960):

$$\tilde{\boldsymbol{T}} = -(\tilde{p} + \tfrac{1}{2}\epsilon\tilde{E}^2)\boldsymbol{I} + \epsilon\tilde{\boldsymbol{E}}\tilde{\boldsymbol{E}}. \tag{6}$$

2.2. *Governing equations and boundary conditions*

When gravitational and electrical forces are vanishingly small compared to surface tension forces, equilibrium drop shapes are segments of spheres and are conveniently parametrized in terms of the single parameter d, the signed distance from the centre of the sphere to the plate, or its ratio to the radius of the sphere, i.e. $D \equiv d/R$. When $D = 0$ the drop is a hemisphere; when $D > 0$ the drop is larger than a hemisphere; when $D < 0$ the drop is smaller than a hemisphere. Equations that follow are made dimensionless by measuring length in units of R, potential U in units of u_0. Hence

$$\boldsymbol{\nabla} \equiv R\tilde{\boldsymbol{\nabla}}, \quad U \equiv \frac{\tilde{U}}{u_0}, \quad \boldsymbol{E} \equiv \frac{R\tilde{\boldsymbol{E}}}{u_0}, \quad \boldsymbol{D} \equiv \frac{R\tilde{\boldsymbol{D}}}{\epsilon_0 u_0}, \quad \boldsymbol{P} \equiv \frac{R\tilde{\boldsymbol{P}}}{\epsilon_0 u_0}. \tag{7}$$

A variable appearing with a tilde above it is dimensional; without a tilde it is dimensionless.

From (2), the electric field $\boldsymbol{E} = -\boldsymbol{\nabla}U$ both outside and inside the drop. Then from (1) and (3) it follows that the potential is governed by the linear Laplace equation outside the drop

$$\boldsymbol{\nabla}^2 U^{(a)} = 0 \quad \text{in} \quad V_a \tag{8}$$

and by a nonlinear partial differential equation inside it

$$\boldsymbol{\nabla}\cdot\left[\left(1 + \frac{P^{(b)}}{E^{(b)}}\right)\boldsymbol{\nabla}U^{(b)}\right] = 0 \quad \text{in} \quad V_b. \tag{9}$$

Subscripts and superscripts a and b denote the exterior and interior of the drop, respectively.

The drop shape is unknown *a priori* and is governed by the augmented Young–Laplace equation, the requisite balance between surface tension, gravitational, and electrical forces:

$$-2\mathscr{H} = K - Gz + N_e H^2 \left[\kappa_a E_n^{(a)2} + E_n^{(b)2} - (\kappa_a - 1) E_t^2 + 2 \int_0^{E^{(b)}} P \, dE - 2 E_n^{(b)} D_n^{(b)} \right] \quad \text{on} \quad S_S, \quad (10)$$

where S_S is the drop surface. Equation (10) results when (5) for the stress tensor of the fluid in the drop and (6) for that outside are substituted into the normal stress boundary condition. $2\mathscr{H}$ is twice the local mean curvature of the interface and is the negative of the surface divergence of the field of unit normals to the drop surface, i.e. $2\mathscr{H} = -\nabla_S \cdot \boldsymbol{n}_S$. The distance z is measured from the origin in the direction opposite to gravity; reference pressure $K \equiv R\Delta p_0/\sigma$ is simply the pressure excess at the level of the plane called $z = 0$ in the drop, measured in units of half the capillary pressure within an uncharged spherical drop of radius R. E_n and E_t are the normal and tangential components, respectively, of the electric field at the drop surface, where $E_n^{(a)} \neq E_n^{(b)}$ but $E_t^{(a)} = E_t^{(b)} = E_t$, as shown below. D_n is the normal component of the electric displacement at the drop surface. $\kappa_a \equiv \epsilon_a/\epsilon_0$ is the ratio of the permittivity of the material surrounding the drop to the permittivity of free space, otherwise known as the dielectric constant of the ambient fluid. $N_e \equiv \epsilon_0 R u_0^2/(2\sigma h^2)$ is the electric bond number; $H = h/r$ is the dimensionless plate separation. The quantity

$$(N_e \kappa_a)^{\frac{1}{2}} = (u_0/h)(\epsilon_a R/2\sigma)^{\frac{1}{2}}$$

is the dimensionless parallel-plate electric field strength. In most situations of practical interest, the ambient fluid is virtually non-polarizable (or non-magnetizable), e.g. air. Therefore, it is supposed in §3 that $\epsilon_a = \epsilon_0$ or $\kappa_a = 1$. It is also supposed in §3 that the effect of gravity is far less than that of surface tension, i.e. the gravitational bond number $G \equiv gR^2\Delta\rho/\sigma$ is vanishingly small, where g is the acceleration due to gravity and $\Delta\rho$ the density difference between the drop and surrounding fluid. When $G \to 0$, K is simply the dimensionless excess pressure in the drop over ambient pressure. The reference pressure K is set by constraining the drop volume to be a fixed amount V_0:

$$V = V_0. \quad (11)$$

The governing equations (8), (9), and (10) are solved subject to the boundary conditions

$$\boldsymbol{n}_S \times \boldsymbol{e}_z = 0 \text{ at } z = a \quad \text{along } S_{\text{sym}}, \quad (12)$$

$$\delta\theta_C = \delta[\cos^{-1}(\boldsymbol{n}_S \cdot \boldsymbol{n}_B)] = 0 \quad \text{or} \quad \delta \boldsymbol{x}_S = 0 \quad \text{at} \quad z = 0, \quad (13a, b)$$

$$U = 1 \quad \text{on} \quad S_{\text{bottom}}, \quad (14)$$

$$U = 0 \quad \text{on} \quad S_{\text{top}}, \quad (15)$$

$$\boldsymbol{n} \cdot \nabla U = 0 \quad \text{on} \quad S_{\text{sym}} \quad \text{and} \quad S_{\text{asym}}, \quad (16)$$

$$E_t^{(a)} = E_t^{(b)} \equiv E_t \quad \text{or} \quad U^{(a)} = U^{(b)} \quad \text{on} \quad S_S, \quad (17)$$

$$D_n^{(a)} = D_n^{(b)} \quad \text{or} \quad \kappa_a E_n^{(a)} = \left(1 + \frac{P^{(b)}}{E^{(b)}}\right) E_n^{(b)} \quad \text{on} \quad S_S, \quad (18)$$

where $\boldsymbol{e}_z$ is a unit vector and a is the length of the drop in the z-direction. Equation (12) ensures that the drop profile remains axially symmetric as it deforms. Equation (13) is the boundary condition at the contact line (circle), where $\boldsymbol{x}_S \in S_S$, θ_c is the contact angle and $\boldsymbol{n}_B$ is the unit normal to the bottom plate. Equation (13a) is the fixed-contact-angle condition and (13b) is the fixed-contact-line condition. Equations (14) and (15) ensure that the potentials of the two solid plates are uniform because they are conducting surfaces. Equation (16) is the condition that the electrostatic field and potential be axially symmetric and that far from the drop the field asymptotically approach a vertically directed uniform field which has strength $1/H$. Equations (17) and (18) are the conditions that the tangential component of the electric field and the normal component of the electric displacement be continuous across the interface (see e.g. Landau & Lifshitz 1960).

2.3. *Constitutive equation for polarization*

The equation set is closed by means of a constitutive equation for polarization:

$$P = \alpha\left[\coth(\tau E) - \frac{1}{\tau E}\right]. \tag{19}$$

The Langevin equation (19) is the simplest form of a constitutive equation frequently used to describe the polarizability of magnetically susceptible fluids (Rosensweig 1985). The physical meanings of the parameters α and τ can be understood by examining the asymptotic behaviour of P for small and large values of E while holding α and τ fixed:

$$\lim_{E\to 0} P = \tfrac{1}{3}\alpha\tau E, \tag{20}$$

$$\lim_{E\to\infty} P = \alpha. \tag{21}$$

The product $\frac{1}{3}\alpha\tau$ is the initial slope of the curve relating polarization to field strength; α is the saturation polarization and τ is a growth constant. Figure 3 shows how the polarization P varies with field strength E as a function of α and τ, when the product $\alpha\tau$ is held fixed at 120. In §3, theoretical predictions are reported for nonlinearly polarizable drops for which $\alpha\tau = 120$. The dimensionless form of (3) is

$$\boldsymbol{D} = \kappa\boldsymbol{E} = \boldsymbol{E} + \boldsymbol{P}, \tag{22}$$

where $\kappa = \kappa(\boldsymbol{E}^2) = \epsilon/\epsilon_0$. Therefore, when $E \to 0$, a nonlinearly polarizable material behaves like a linear material with $\kappa = 1 + \frac{1}{3}\alpha\tau$.

Using expression (19) for the polarization, the Young–Laplace equation (10) can be rewritten as

$$-2\mathscr{H} = K - Gz + N_e H^2\left\{\kappa_a E_n^{(a)2} - (\kappa_a - 1)E_t^2 + 2\frac{\alpha}{\tau}\log\left[\sinh(\tau E^{(b)})/(\tau E^{(b)})\right] - 2\left(\frac{1}{2} + \frac{P^{(b)}}{E^{(b)}}\right)E_n^{(b)2}\right\}. \tag{23}$$

Were the drop a linear material, (23) would then reduce to (cf. W & B)

$$-2\mathscr{H} = K - Gz + N_e \kappa_a H^2\left\{E_n^{(a)2} - \frac{\kappa_b}{\kappa_a}E_n^{(b)2} + \left(\frac{\kappa_b}{\kappa_a} - 1\right)E_t^2\right\}, \tag{24}$$

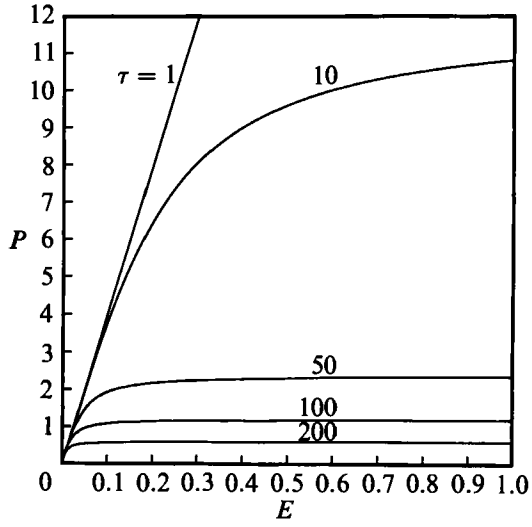

FIGURE 3. Variation of polarization, P, with electric field strength, E, when $\alpha\tau = 120$.

where the dielectric constant $\kappa_b \equiv \epsilon_b/\epsilon_0$ is a constant. W & B analysed the response of supported drops as a function of $N_{e,WB} \equiv N_e\kappa_a$ for various values of $\kappa_{WB} \equiv \kappa_b/\kappa_a = \epsilon_b/\epsilon_a$. Because $\kappa_a = 1$ in this paper, the results of W & B are readily recovered here by identifying κ_b in this paper with their κ_{WB} and N_e in this paper with their $N_{e,WB}$.

3. Results

Figure 4 shows how the aspect ratio of drops making a fixed contact angle of 90° ($D = 0$) with the supporting plate varies with parallel-plate field strength $\bar{N}_e$. One of the curves shown is for a linearly polarizable drop with $\kappa = 41$; all others are for nonlinearly polarizable drops for which the product $\alpha\tau = 120$. The response of the nonlinearly polarizable drop with $\alpha = 12$, $\tau = 10$ is identical to that of the linearly polarizable drop: the two curves lie on top of one another. These two shape families are stable up to the turning point and unstable beyond it (cf. W & B). The end points of these two curves represent termination of these two shape families, where the mean curvature at the drop tip tends to infinity (Miksis 1981, cf. W & B). The response of nonlinearly polarizable drops for which $\tau < 10$ is also identical to that of the linearly polarizable drop; these curves are not shown in figure 4. When τ is increased to 50, the response of the nonlinearly polarizable drop differs only slightly from that of the linearly polarizable drop. Nevertheless, the response is qualitatively unchanged, i.e. there is loss of stability at the turning point with respect to field strength and this shape family with $\tau = 50$ also terminates at the largest aspect ratio shown. When τ is increased to 100, there is little quantitative difference in the response of the nonlinearly polarizable drop from that of the linearly polarizable drop for drop aspect ratios as high as 3.5. Indeed, the value of the field strength at the first turning point along the curve corresponding to $\tau = 100$ differs by less than 0.4% from that at the turning point along the curve corresponding to the linearly polarizable drop. However, the qualitative response of these two drops is radically different: the shape family of nonlinearly polarizable drops with $\tau = 100$ has a second turning point with respect to field strength at which it regains stability with respect

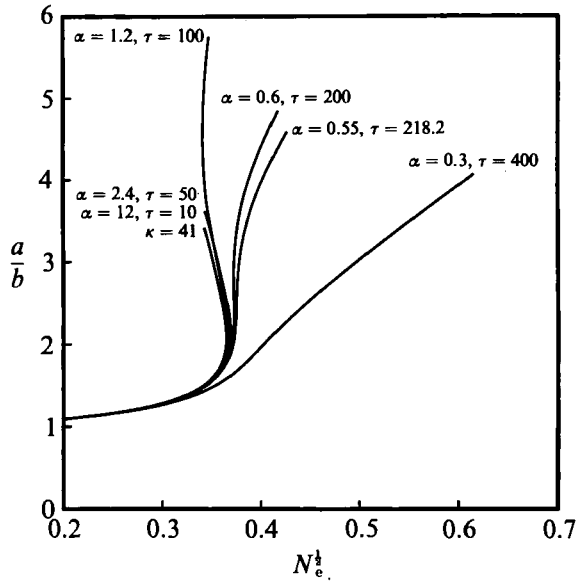

FIGURE 4. Variation of aspect ratio a/b with field strength for initially hemispherical drops ($D = 0$) whose contact angles are prescribed. For nonlinearly polarizable drops, the product $\alpha\tau = 120$. The drop deformation curve for a linearly polarizable drop with $\kappa = 41$ is also shown for comparison. Here the plate spacing $H = 20$.

to perturbations having an infinitesimal amplitude. Thus, this shape family exhibits hysteresis in drop deformation, similar to that reported earlier by W & B for linearly polarizable drops when the value of κ falls within some range. Moreover, that this hysteresis behaviour exists over a wide range of values of α and τ can also be seen from figure 4, cf. the shape family for which $\alpha = 0.6$ and $\tau = 200$. Finally, as the value of τ is further increased, or the value of α is further decreased, the response becomes one in which drop deformation, or aspect ratio, increases monotonically with field strength, cf. the shape families for which $\alpha = 0.55$ and $\tau = 120/0.55 \doteq 218.2$ and $\alpha = 0.3$ and $\tau = 400$.

Figure 5 shows the evolution of shapes of drops that are members of the families depicted in figure 4, which are constrained to meet the supporting plate at a fixed contact angle of 90°, with increasing drop deformation. Plainly, up to an aspect ratio of about 3, the drop shapes in figures 5(*a*)–5(*c*) are remarkably similar. When the aspect ratio exceeds the value it has at the turning point, the contact line of the linearly polarizable drop moves only slightly: see figure 5(*a*). Indeed, for $3 < a/b < 3.4$, the contact line almost behaves as though it were pinned on the solid support. This fact may explain why the mean curvature at the drop tip rapidly grows without bound for $a/b \approx 3.4$ and the family of linearly polarizable drops of $\kappa = 41$ ends shortly thereafter. By contrast, the contact line of the nonlinearly polarizable drop shown in figure 5(*b*) continuously recedes as the drop deforms: this permits the formation of highly elongated shapes and of virtually conical drop tips of increasing local mean curvature. The last drop shape shown in figure 5(*b*), with an aspect ratio of 5, lies along the upper stable branch of the shape family with $\alpha = 1.2$, $\tau = 100$ that is shown in figure 4. The nonlinearly polarizable drop whose shapes are shown in figure 5(*c*) behaves similarly to that shown in figure 5(*b*). However, there are some important differences in the response of these two nonlinearly polarizable drops as well. Figure 3 makes plain that the drop of figure 5(*c*) saturates more readily with the

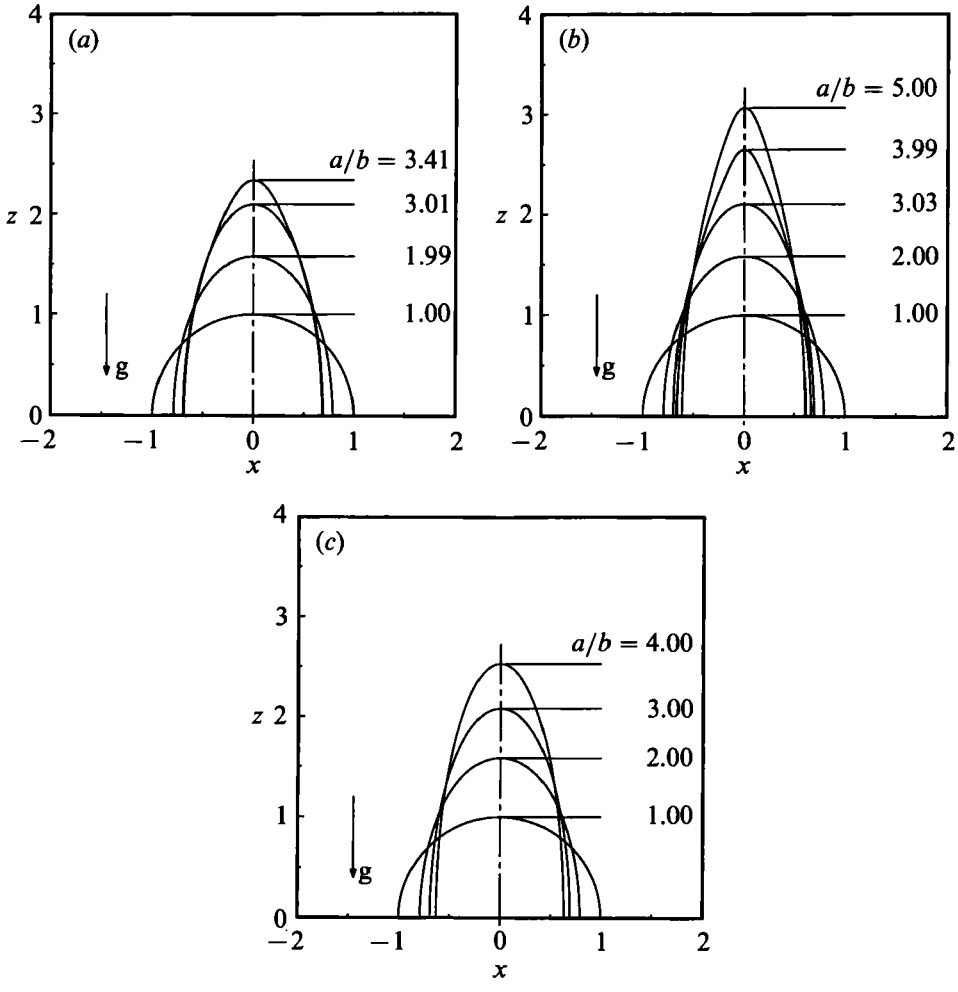

FIGURE 5. Shapes of axisymmetric supported drops when $D = 0$, $G = 0$ and $H = 20$; fixed-contact-angle case. (*a*) Linearly polarizable drop with $\kappa = 41$. Values of the parallel-plate electric field strength $N_e^{\frac{1}{2}}$ corresponding to the aspect ratios shown are 0 for $a/b = 1$, 0.3643 for $a/b = 1.99$, 0.3509 for $a/b = 3.01$, and 0.3423 for $a/b = 3.41$. (*b*) Nonlinearly polarizable drop with $\alpha = 1.2$ and $\tau = 100$. Values of the parallel-plate electric field strength $N_e^{\frac{1}{2}}$ corresponding to the aspect ratios shown are 0 for $a/b = 1$, 0.3656 for $a/b = 2$, 0.3548 for $a/b = 3.03$, 0.3426 for $a/b = 3.99$, and 0.3418 for $a/b = 5$. (*c*) Nonlinearly polarizable drop with $\alpha = 0.3$ and $\tau = 400$. Values of the parallel-plate electric field strength $N_e^{\frac{1}{2}}$ corresponding to the aspect ratios shown are 0 for $a/b = 1$, 0.4021 for $a/b = 2$, 0.4978 for $a/b = 3$, and 0.6078 for $a/b = 4$.

applied field than the drop of figure 5(*b*). As τ increases and α decreases, while keeping their product constant, as in going from figure 5(*b*) to 5(*c*), the polarizability of a nonlinearly polarizable drop approaches that of the ambient fluid outside it. Indeed, for sufficiently large (small) values of τ (α) a situation is reached in which the electric field everywhere between the plates – inside as well as outside the drop – is virtually $(1/H)\,\boldsymbol{e}_z$. Consequently, the tips of drops in figure 5(*c*) are more rounded than those of drops in figure 5(*b*) even at large deformations: compare the tips of drops in figures 5(*b*) and 5(*c*) at an aspect ratio of 4. Moreover, one would expect the drop of figure 5(*c*) to undergo a smaller deformation than the drop of figure 5(*b*) when compared at the same value of the applied field strength: this conclusion too accords with the deformation response of the shape families depicted in figure 4.

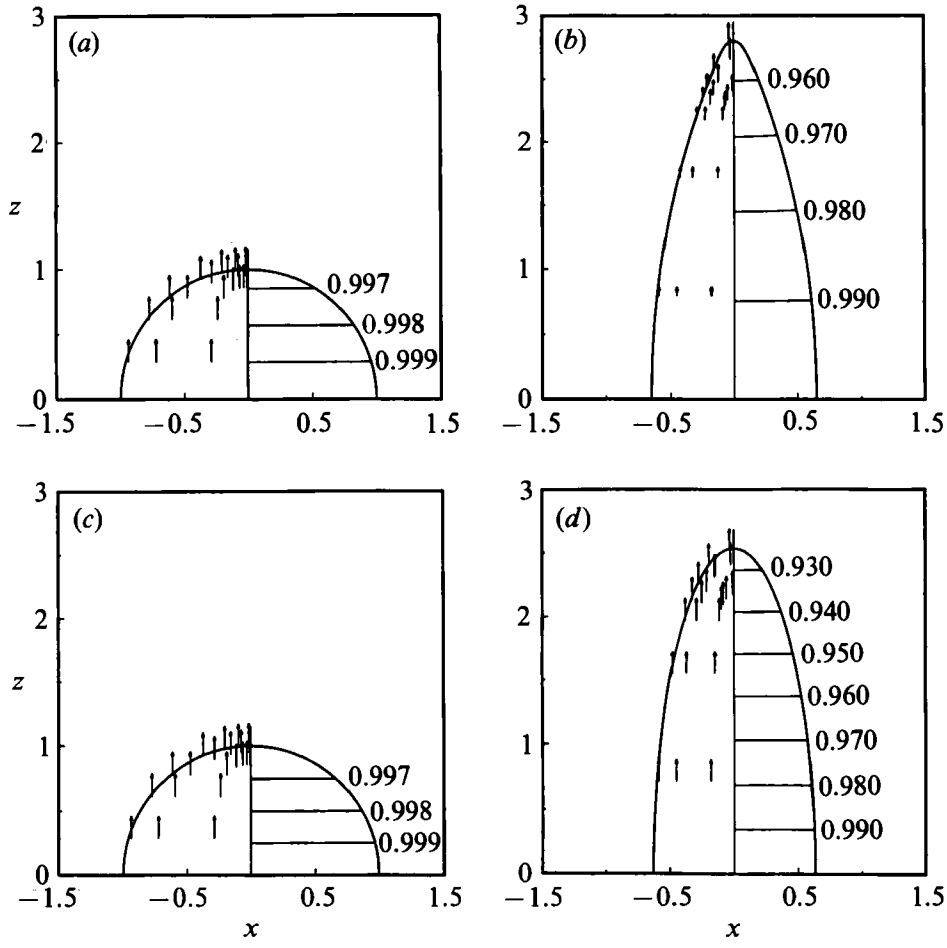

FIGURE 6. Drop shapes, equipotentials, and electric field vectors inside nonlinearly polarizable drops whose contact angles are fixed when $D = 0$, $G = 0$ and $H = 20$. (*a*) $\alpha = 1.2$, $\tau = 100$, $a/b = 1.0$ and $N_e^{\frac{1}{2}} = 0$; (*b*) $\alpha = 1.2$, $\tau = 100$, $a/b = 4.3$ and $N_e^{\frac{1}{2}} = 0.3412$; (*c*) $\alpha = 0.3$, $\tau = 400$, $a/b = 1.0$ and $N_e^{\frac{1}{2}} = 0$; (*d*) $\alpha = 0.3$, $\tau = 400$, $a/b = 4.0$ and $N_e^{\frac{1}{2}} = 0.6088$.

To gain further insight into the underlying physics, it is instructive to examine the electric field vectors and equipotential lines inside nonlinearly polarizable drops. Figure 6 shows the evolution with increasing drop deformation of the electric field and equipotential lines inside initially hemispherical, nonlinearly polarizable drops whose contact angles are fixed. In figures 6(*a*) and 6(*b*) $\alpha = 1.2$ and $\tau = 100$, and in figures 6(*c*) and 6(*d*) $\alpha = 0.3$ and $\tau = 400$. Figures 6(*a*) and 6(*b*) show that the field inside a drop having an $O(1)$ value of α becomes non-uniform as drop deformation increases. This stands in contrast to drops that are linearly polarizable (W & B), and, not too surprisingly, also to ones which have a large enough value of α or a small enough value of the growth constant τ, inside which the field is virtually uniform at all aspect ratios (not shown here). As figures 6(*a*) and 6(*c*) show, the field inside hemispherical drops is uniform regardless of the values of α and τ. What is unclear is how the field behaves as the saturation polarization α is lowered, or the growth constant τ is raised. Figure 6(*d*) shows the electric field and equipotential lines inside a drop which is more readily saturated than the one in figure 6(*b*) so that its aspect ratio versus field strength curve does not exhibit hysteresis (cf. figure 4). Clearly, the

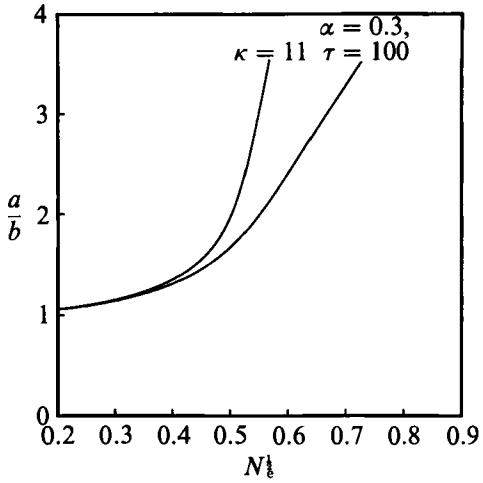

FIGURE 7. Variation of aspect ratio a/b with field strength of initially hemispherical drops ($D = 0$) whose contact angles are prescribed. Here the plate spacing $H = 20$. For nonlinearly polarizable drops, the product $\alpha\tau = 30$. The deformation curve for a linearly polarizable drop with $\kappa = 11$ is also shown for comparison.

field inside the drop is virtually uniform at an aspect ratio as high as 4. However, the field strength inside does not remain constant as the relative importance of electrical forces to surface tension forces increases. The field strength inside the drop increases from approximately 0.004 when $N_e^{\frac{1}{2}} = 0$ to 0.028 when $N_e^{\frac{1}{2}} = 0.6088$.

Figure 7 shows how the aspect ratio of drops making a fixed contact angle of 90° ($D = 0$) with the supporting plate varies with parallel-plate field strength $N_e^{\frac{1}{2}}$. One of the curves shown is for a linearly polarizable drop with $\kappa = 11$ and the other is for a nonlinearly polarizable drop for which the product $\alpha\tau = 30$. W & B have shown that the aspect ratio of the linear dielectric drop with $\kappa = 11$ increases monotonically with N_e. Figure 7 makes plain that the effect of increasing nonlinearity in polarization, i.e. increasing τ and decreasing α, is to make the aspect ratio versus field strength curves flatter while leaving the qualitative response unchanged in comparison to the linearly polarizable drop. Figures 4 and 7 both demonstrate the big role that nonlinear polarization can play in determining the response of real drops.

Figure 8 shows how the aspect ratio of drops making a fixed contact angle of approximately 37° ($D = 0.8$) with the supporting plate varies with parallel-plate field strength $N_e^{\frac{1}{2}}$. One of the curves shown is for a linearly polarizable drop with $\kappa = 41$ and the other is for a nonlinearly polarizable drop for which the product $\alpha\tau = 120$. In the limiting case of the linearly polarizable drop, the drop deformation increases with field strength up to the turning point and the shape family terminates shortly thereafter, as shown in figure 8. By contrast, for the nonlinearly polarizable drop the deformation versus field strength curve is not only flatter than that of the linearly polarizable drop, but exhibits hysteresis as well. Thus, proper accounting for the nonlinear polarization of the drop material has allowed theoretical prediction of hysteresis in drop deformation for drops having a wide variety of wetting properties with the solid support (i.e. in situations in which the contact angle is not necessarily 90°). Moreover, the methodology of this paper and the new predictions can provide guidance to future experiments with fluids having arbitrary wetting properties with the supporting plate.

Figure 9 shows the electric field and equipotential lines inside drops that meet the

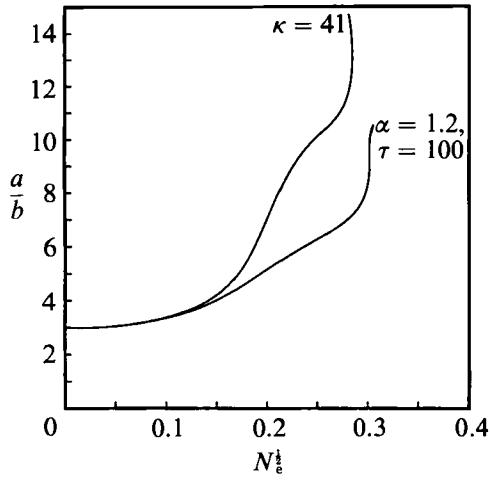

FIGURE 8. Variation of aspect ratio a/b with field strength for drops having a volume larger than a hemisphere and whose contact angles are prescribed. Here the drop size parameter $D = 0.8$ and the plate separation $H = 20$. For nonlinearly polarizable drops, the product $\alpha\tau = 120$. The deformation curve for a linearly polarizable drop with $\kappa = 41$ is also shown for comparison.

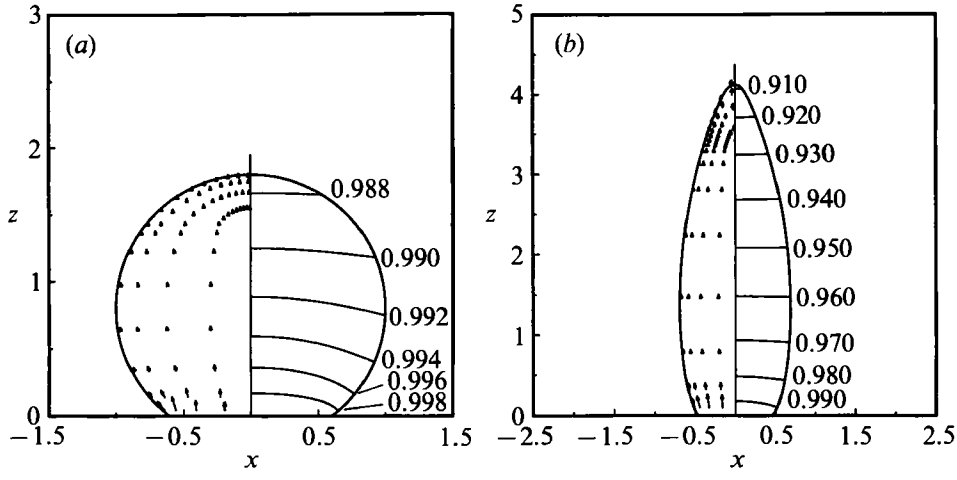

FIGURE 9. Drop shapes, equipotentials, and electric field vectors inside drops having a volume larger than a hemisphere and whose contact angles are prescribed. Here $\alpha = 1.2$, $\tau = 100$, $D = 0.8$, and $H = 20$. (a) $a/b = 3.0$ and $N_e^{\frac{1}{2}} = 0$, (b) $a/b = 9.0$ and $N_e^{\frac{1}{2}} = 0.3026$.

supporting plate at a fixed contact angle that differs from 90°. The drops shown in figure 9 have nonlinear polarization parameters $\alpha = 1.2$ and $\tau = 100$. When the contact angle is approximately 37° ($D = 0.8$) the field is highly non-uniform inside the 'fat' drop even when it is undeformed ($N_e^{\frac{1}{2}} \to 0$) and is strongest at the bottom (see figure 9a). In contrast to hemispherical drops, the electric field vectors inside such large drops are not parallel to the applied field near the bottom of the drop and tend to point away from the axis of symmetry. Figure 9(b) shows the evolution with field strength of the shape and the electric field inside the nonlinearly polarizable drop down in figure 9(a). As such a fat drop deforms, the field near its tip increases, as in an initially hemispherical drop having the same values of α and τ (recall figure 6b). However, the field near the bottom plate inside the drop is still larger than the field anywhere else inside it. Remarkably, a region of weak field strength develops in the

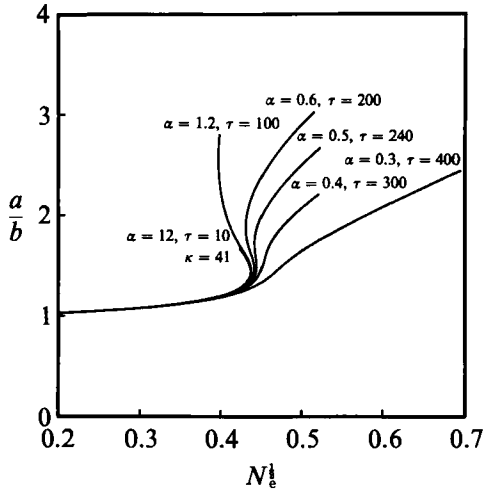

FIGURE 10. Variation of aspect ratio a/b with field strength for initially hemispherical drops ($D = 0$) whose contact lines are fixed. For nonlinearly polarizable drops, the product $\alpha\tau = 120$. The deformation curve for a linearly polarizable drop with $\kappa = 41$ is also shown for comparison. Here the plate spacing $H = 20$.

centre of the drop, between its tip and the bottom plate. The complexity of the fields inside and outside such drops, in contrast to simple spheroids, makes plain the dangers of using *ad hoc* models such as the spheroidal approximation instead of rigorous computer-aided means in analysing the response of supported drops.

Figure 10 shows how the aspect ratio of drops whose contact lines are fixed varies with parallel-plate field strength $N_e^{\frac{1}{2}}$. One of the curves shown is for a linearly polarizable drop with $\kappa = 41$; all others are for nonlinearly polarizable drops for which the product $\alpha\tau = 120$. The response of the nonlinearly polarizable drop with $\alpha = 12$, $\tau = 10$ is identical to that of the linearly polarizable drop: the two curves lie on top of one another. These two shape families are stable up to the turning point and unstable beyond it (cf. W & B). The end points of these two curves represent termination of these two shape families, where the mean (radius of) curvature at the drop tip tends to infinity (zero). When $\tau < 10$, the response of nonlinearly polarizable drops whose contact lines are fixed, as well as ones whose contact angles are prescribed (cf. figure 4), are identical to those of linearly polarizable drops obeying the same contact line boundary condition with the solid support. When τ is increased to 100, there is little quantitative difference in the response of the nonlinearly polarizable drop from that of the linearly polarizable drop for small to moderate drop aspect ratios. However, the qualitative response of these two drops is radically different: the shape family of nonlinearly polarizable drops with $\tau = 100$ has a second turning point with respect to field strength at which it regains stability with respect to all axisymmetric perturbations having an infinitesimal amplitude. Thus this shape family exhibits hysteresis in drop deformation. Moreover, this hysteresis behaviour exists over a wide range of values of α and τ, as shown in figure 10. As the value of τ is further increased, or the value of α is further decreased, the response becomes one in which drop deformation, or aspect ratio, increases monotonically with field strength, cf. the shape families for which $\alpha = 0.4$ and $\alpha = 0.3$. Figures 10 and 4 make plain that fixing the contact line of a drop, instead of prescribing its contact angle, widens the range of values of α, or τ, when the product $\alpha\tau$ is fixed, over which hysteresis can be observed. Whereas a drop having Langevin parameters $\alpha = 0.5$ and

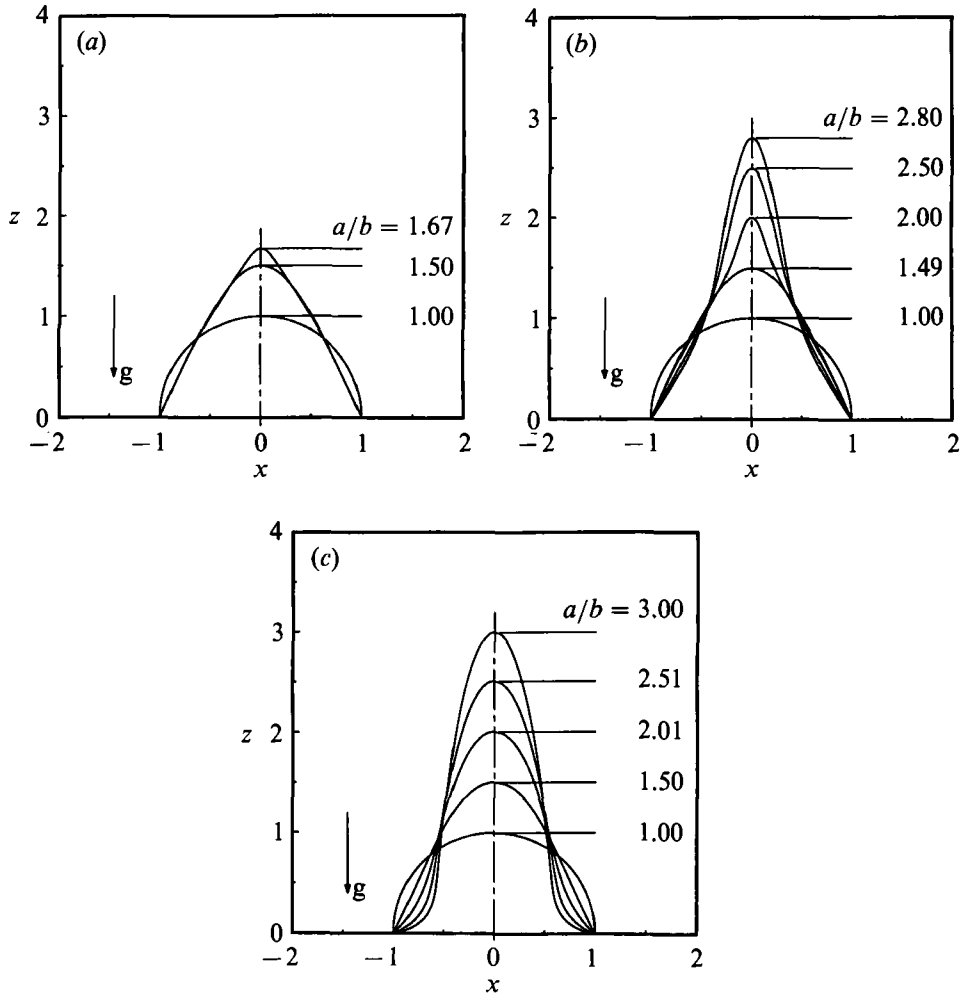

FIGURE 11. Shapes of axisymmetric supported drops when $D = 0$, $G = 0$ and $H = 20$; fixed-contact-line case. (*a*) Linearly polarizable drop with $\kappa = 41$. (*b*) Nonlinearly polarizable drop with $\alpha = 1.2$ and $\tau = 100$. (*c*) Nonlinearly polarizable drop with $\alpha = 0.3$ and $\tau = 400$.

$\tau = 240$ exhibits hysteresis in deformation when its contact line is fixed, a drop having a higher value of α (and a lower value of τ) e.g. $\alpha = 0.55$ and $\tau = 218.2$, does not when its contact angle is fixed.

Figure 11 shows the evolution of shapes of drops that are members of the families depicted in figure 10, which make a fixed contact line with the supporting plate, with increasing drop deformation. Plainly, up to an aspect ratio of about 1.5, the drop shapes are remarkably similar. When the aspect ratio exceeds the value it has at the turning point, increasing nonlinearity of drop polarization results in large differences in drop profiles. In the family of linearly polarizable drops, a drop shape having a virtually conical tip is shown in figure 11 (*a*): this shape is reminiscent of the conical drop whose existence was first suggested by Taylor (1964). However, figures 11 (*b*) and 11 (*c*) show that as the nonlinearity of fluid polarization increases, the drop profiles become concave near their bases at large drop deformations.

4. Conclusions

In a series of experiments with ferrofluid drops, Bacri *et al.* (1982) and Bacri & Salin (1982, 1983) reported observing hysteresis in deformation with drops that were assumed to be linearly polarizable ferrofluids with $\kappa \approx 40$. However, this value of κ was not measured directly, but was back calculated from a fit of the observed hysteresis curve to that predicted by using a spheroidal approximation of drop shapes. Results presented in this paper for a nonlinearly polarizable drop with a fixed contact angle of 90°, corresponding to the case of a free drop, which initially behaves like a linearly polarizable drop with $\kappa = 41$ are in excellent agreement with these experiments. Indeed, there is a wide range of values of the Langevin parameters α and τ over which hysteresis ought to be observed.

According to the results of this paper, nonlinear polarization plays an increasingly dominant role in determining the qualitative response of a drop as its deformation increases. However, because of the similarities in behaviour between linearly and nonlinearly polarizable materials at low and even moderate field strengths, indeed often nearly identical behaviour up to the first stability limit, it is recommended that future experimental work place a larger emphasis on the measurement and characterization of the nonlinear polarization of the drop material.

Moreover, fixing the contact line of a drop instead of prescribing its contact angle widens the window of opportunity for observing hysteresis for drops that are linearly polarizable (see W & B) and ones that are nonlinearly polarizable as well. Thus, future experiments in which pendant or sessile drops are emanating from a nozzle may offer new opportunities for observing hysteresis phenomena.

This research was sponsored by the Division of Chemical Sciences, Office of Basic Energy Sciences (BES), US Department of Energy (DOE) under contract DE-AC05-84OR21400 with Martin Marietta Energy Systems, Inc. Calculations were carried out at the Florida State University (FSU) Computing Center under a grant from the BES Office of the US DOE. S. A. Kaye, a participant in the Oak Ridge Science and Engineering Research Semester (ORSERS) program, helped in the preparation of the figures for this article. The authors thank the referees for their constructive comments regarding this manuscript.

REFERENCES

Bacri, J. C. & Salin, D. 1982 Instability of ferrofluid magnetic drops under magnetic field. *J. Phys. Lett.* **43**, L649.

Bacri, J. C. & Salin, D. 1983 Dynamics of the shape transition of a ferrofluid magnetic drop. *J. Phys. Lett.* **44**, L415.

Bacri, J. C., Salin, D. & Massart, R. 1982 Shape of the deformation of ferrofluid droplets in a magnetic field. *J. Phys. Lett.* **43**, L179.

Basaran, O. A. 1984 Electrohydrodynamics of drops and bubbles. PhD thesis, University of Minnesota, Minneapolis.

Berkovsky, B. M. & Kalikmanov, V. I. 1985 Topological instability of magnetic fluids. *J. Phys. Lett.* **46**, L483.

Boudouvis, A. G., Puchalla, J. L. & Scriven, L. E. 1988 Magnetohydrostatic equilibria of ferrofluid drops in external magnetic fields. *Chem. Engng Commun.* **67**, 129.

Cheng, K. J. & Miksis, M. J. 1989 Shape and stability of a drop on a conducting plane in an electric field. *PhysicoChem. Hydrodyn.* **11**, 9.

Landau, L. D. & Lifshitz, E. M. 1960 *Electrodynamics of Continuous Media.* Pergamon.

Melcher, J. R. 1981 *Continuum Electromechanics.* MIT Press.

MELCHER, J. R. & TAYLOR, G. I. 1969 Electrohydrodynamics: a review of the role of interfacial shear stresses. *Ann. Rev. Fluid Mech.* **1**, 111.

MIKSIS, M. J. 1981 Shape of a drop in an electric field. *Phys. Fluids* **24**, 1967.

ROSENKILDE, C. E. 1969 A dielectric fluid drop in an electric field. *Proc. R. Soc. Lond.* A **312**, 473.

ROSENSWEIG, R. E. 1979 Fluid dynamics and science of magnetic liquids. In *Advances in Electronics and Electron Physics*, vol. 48 (ed. L. Marton). Academic.

ROSENSWEIG, R. E. 1985 *Ferrohydrodynamics*. Cambridge University Press.

SHERWOOD, J. D. 1988 Breakup of fluid droplets in electric and magnetic fields. *J. Fluid Mech.* **188**, 133.

TAYLOR, G. I. 1964 Disintegration of water drops in an electric field. *Proc. R. Soc. Lond.* A **280**, 383.

WOHLHUTER, F. K. & BASARAN, O. A. 1992 Shapes and stability of pendant and sessile dielectric drops in an electric field. *J. Fluid Mech.* **235**, 481 (referred to herein as W & B).